Applied Catalysis B: Environmental 100 (2010) 205–211

Contents lists available at ScienceDirect

Applied Catalysis B: Environmental

journal homepage: www.elsevier.com/locate/apcatb

Low-temperature carbon combustion over proton conductor + electrocatalyst-mixed powders

Kota Tsuneyama [a], Yosuke Sakamoto [b], Kenzi Suzuki [b], Takashi Hibino [a,*]

[a] Graduate School of Environmental Studies, Nagoya University, Furo-cho, Chikusa-ku, Nagoya 464-8601, Japan
[b] Ecotopia Science Institute, Nagoya University, Nagoya 464-8603, Japan

ARTICLE INFO

Article history:
Received 18 June 2010
Received in revised form 22 July 2010
Accepted 29 July 2010
Available online 6 August 2010

Keywords:
Carbon oxidation
Active oxygen
Proton conductor
Particulate matter

ABSTRACT

Catalytic carbon combustion is a potential approach for eliminating particulate matter emissions from diesel engine vehicles. In this study, we report low-temperature carbon combustion by active oxygen formed at the interface of the mixed powders of a proton conductor ($Sn_{0.9}In_{0.1}P_2O_7$) and electrocatalyst (Pt or Mo_2C). In a gaseous mixture of H_2O and O_2, H_2O dissociated into protons and electrons at an anodic site of the interface and the resultant active oxygen oxidized carbon to CO_2. Separately, O_2 reacted with protons and electrons to form H_2O at a cathodic site of the interface, resulting in formation of a local electrochemical cell at the proton conductor–electrocatalyst interface, which then self-discharged. This series of reactions could successfully reduce the ignition temperature for carbon to 200 °C for Pt and 300 °C for Mo_2C.

1. Introduction

Diesel engine vehicles have recently become widespread because of their higher efficiency fuel combustion and lower CO_2 emissions compared to gasoline engine vehicles. At the same time, however, hazards to humans due to carbonaceous particulate matter (PM) present in diesel emissions have become a subject of great concern. PM, mainly consisting of soot and soluble organic fractions (SOF), is currently removed by trapping the particles on ceramic filters and then burning them [1–3]. The main challenge of this technology is that the combustion of soot requires high temperatures, of around 500 °C. Consequently, to achieve effective filter regeneration it is necessary to raise the temperature by injecting additional diesel fuel into the exhaust stream, reducing the fuel efficiency of diesel engines.

Catalyzed soot combustion is thought to enable filter regeneration at reduced temperatures, which can be accomplished by impregnating the filter surface with a catalyst [4]. It has been reported that several transition metal oxides [5–7] and rare-earth metal oxides [8–10] can activate O_2 in the gas phase or oxide ions in the lattice via their redox properties, allowing for the ignition of soot at lower temperatures. The catalysts providing such active oxygen species are not commercially available for soot combustion yet because the ignition temperature range of 300–500 °C reported so far is much higher than the exhaust temperature of approximately 200 °C observed for diesel engine cars during town driving.

In this study, our attention was focused on H_2O vapor as an oxygen source and a mixture of proton conductor and electrocatalyst powders as a catalyst. It is known that in phosphoric acid and polymer electrolyte fuel cells (PAFCs [11–13] and PEFCs [14–16]) with carbon-supported Pt electrodes, the support is oxidized by H_2O to CO_2 at high electrode potentials (Eq. (1)):

$$C + 2H_2O \rightarrow CO_2 + 4H^+ + 4e^- \quad \text{at} 0.21\,\text{V vs. NHE} \tag{1}$$

All of the above studies have shown that such carbon oxidation is indeed possible below 200 °C. Several have also shown that these reactions actually occur between 0.6 and 1.0 V vs. NHE [12–14,16], which is lower than the potential for the oxygen reduction reaction (Eq. (2)):

$$O_2 + 4H^+ + 4e^- \rightarrow 2H_2O \quad \text{at} 1.23\,\text{V vs. NHE} \tag{2}$$

Thus, it is expected that carbon can be oxidized as in Eqs. (1) and (2), not only at temperatures comparable to typical exhaust temperatures but also in the fuel cell mode, without using an external power source (Scheme 1a). Moreover, if micro-scale electrochemical cells are successfully constituted by mixing proton conductor powder with electrocatalyst powder, the reaction area for carbon oxidation can be drastically increased (Scheme 1b). This paper demonstrates that reactions in Eqs. (1) and (2) are applicable to carbon oxidation, which opens up a new route for the development of soot combustion catalysts.

Proton conductors are important contributing materials for the present purpose. We used $Sn_{0.9}In_{0.1}P_2O_7$ as a proton conductor

* Corresponding author. Tel.: +81 52 789 4888; fax: +81 52 789 4894.
E-mail address: hibino@urban.env.nagoya-u.ac.jp (T. Hibino).

0926-3373/$ – see front matter © 2010 Elsevier B.V. All rights reserved.
doi:10.1016/j.apcatb.2010.07.032

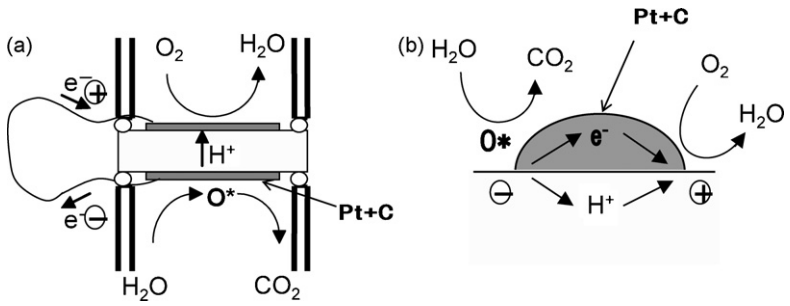

Scheme 1. Reaction schemes of carbon oxidation over (a) a fuel cell and (b) a local electrochemical cell.

because it shows high proton conductivities (above 0.01 S cm^{-1}) in the temperature range of 50–500 °C [17,18]. Electrocatalysts are also very important materials. We used Pt as a typical electrocatalyst and further examined Mo_2C as a potential alternative material to Pt. First, carbon oxidation through the reaction in Eq. (1) was electrochemically inspected over a Pt + carbon-mixed electrode. Then, observation of the reaction intermediate formed over the electrode was carried out using cyclic voltammetry (CV). Finally, the catalytic activity of a physical mixture of $Sn_{0.9}In_{0.1}P_2O_7$ and Pt or Mo_2C powders for carbon oxidation was evaluated in the presence of H_2O vapor and O_2.

2. Experimental

2.1. Materials

$Sn_{0.9}In_{0.1}P_2O_7$ was prepared in the same manner as reported previously [17,18]. SnO_2 and In_2O_3 (Wako) were mixed with 85% H_3PO_4 and ion-exchanged water and held with stirring at 300 °C until a high viscosity paste was formed. This paste was calcined in an alumina pot at 650 °C for 2.5 h and then ground in a mortar. Black pearl 2000 (BET surface area 1365 $m^2\,g^{-1}$) was used as a carbon sample. The thermal stability of the carbon sample was measured by thermal gravimetric and differential thermal analyses (Shimadzu, DTG-60) at a heating rate of 10 °C min^{-1} in air flowing at 100 mL min^{-1}. Commercially available platinum black and Mo_2C (Wako) were tested as electrocatalysts.

2.2. Electrochemical cell studies

For electrochemical cell studies, the $Sn_{0.9}In_{0.1}P_2O_7$ powder was pressed into pellets (diameter: 12 mm; thickness: about 1.5 mm) under a pressure of 200 MPa. Pt and carbon powders (10 wt% Pt) were ground in the mortar for a few minutes and the mixture was examined as the working electrode unless otherwise stated. A commercial Pt/C electrode (BASF, 4 mg Pt cm^{-2}) was used as the counter electrode. The working and counter electrodes (area: 0.5 cm^2) were attached on opposite sides of the electrolyte, wherein no special binder was used. Two gas chambers were established by placing the cell assembly between two alumina tubes as illustrated in Fig. 1. An Au reference electrode was attached to the side surface of the electrolyte. In all of the experiments, the counter and reference electrodes were exposed to atmospheric air. Note that the potential of the working electrode was denoted in air as the basis point.

The electrochemical oxidation reaction was carried out by feeding 3 vol% H_2O vapor diluted with argon into the working electrode at a flow rate of 30 mL min^{-1}. The current was applied with a galvanostat (Hokuto Denko, HA-501). The concentrations of CO*x* (CO_2 and CO) and O_2 in the outlet gas from the working electrode were analyzed using on-line Varian CP-2002 and Shimadzu GC-8A gas chromatographs, respectively.

Further detailed characteristics of the working electrode were obtained using CV. Again, 3 vol% H_2O vapor diluted with argon was supplied into the working electrode at a flow rate of 30 mL min^{-1}. CV profiles were collected between −0.9 and 0.3 V at a scan rate of 10 mV s^{-1} (Hokuto Denko, HZ-5000).

The open-circuit potential of the working electrode was measured in a mixture feed of 3 vol% H_2O vapor and 21 vol% O_2 in argon at a flow rate of 30 mL min^{-1}. The CO*x* concentrations in the outlet gas from the working electrode were monitored in the same manner as described earlier. Anodic and cathodic polarization curves were measured by supplying 3 vol% H_2O vapor diluted with argon into the Pt + carbon-mixed electrode and 21 vol% O_2 diluted with argon into a pure Pt electrode, respectively, at a flow rate of 30 mL min^{-1}. In both measurements, the potential of the working electrode was recorded vs. the reference electrode using an electrometer (Hokuto Denko, He-104).

2.3. Catalyst studies

For catalytic studies, 5 mg carbon was mixed with 90 mg $Sn_{0.9}In_{0.1}P_2O_7$, 10 mg Pt or 10 mg Mo_2C and 5 mg α-Al_2O_3 in the mortar for a few minutes. The dispersion state of each component in the mixed catalyst was analyzed using scanning electron microscopy (SEM) in conjunction with energy dispersive X-ray (EDX) spectroscopy (Hitachi S-4800). For comparison with the $Sn_{0.9}In_{0.1}P_2O_7$ + Pt-mixed catalyst, a Pt/γ-Al_2O_3 (1 wt% Pt) catalyst, which is used as a standard catalyst at Toyota Motor Corporation, was also tested. The number of reaction sites on the Pt surface was

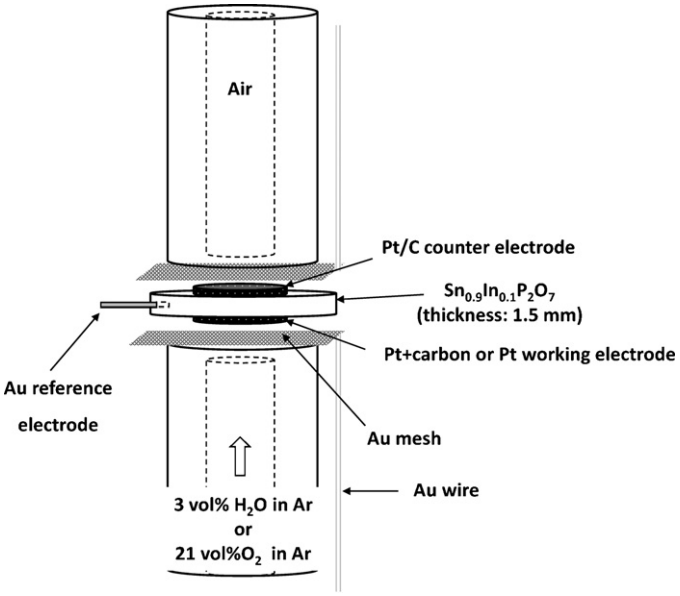

Fig. 1. An illustration of the electrochemical cell.

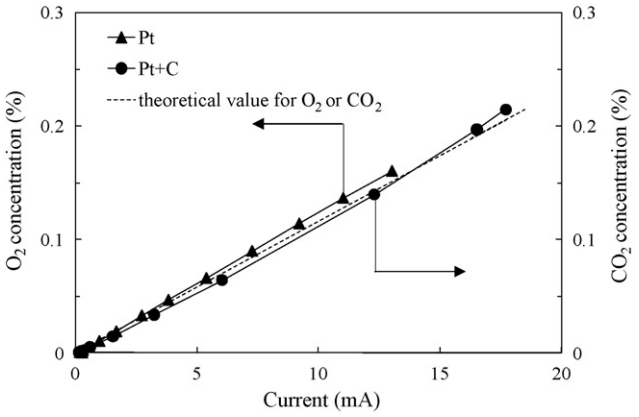

Fig. 2. CO_2 and O_2 concentrations over the Pt + carbon-mixed electrode and Pt electrode in 3 vol% H_2O vapor diluted with argon at 200 °C. The theoretical values calculated from Faraday's law are also included.

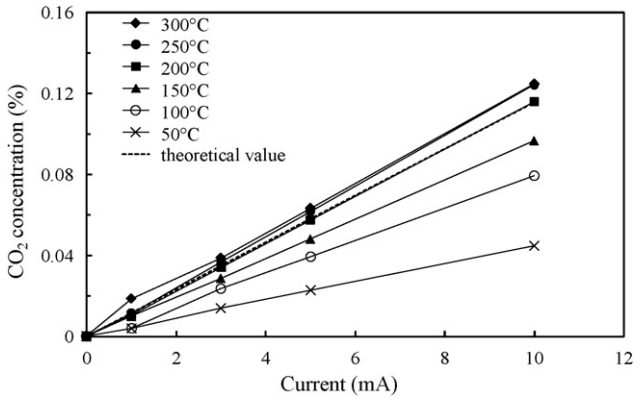

Fig. 3. CO_2 concentration over the Pt + carbon-mixed electrode in 3 vol% H_2O vapor diluted with argon at various temperatures. The theoretical values calculated from Faraday's law are also included.

measured at room temperature using the CO pulse method. Catalytic tests were conducted in a fixed-bed flow reactor. A mixture of ca. 0.01–10 vol% H_2O vapor or 3 vol% D_2O vapor and 21 vol% O_2 in argon was fed into the reactor at a flow rate of 30 mL min^{-1}. Analysis of the outlet gas was carried out in the same manner as described earlier. All experiments were performed from room temperature up to 600 °C.

3. Results and discussion

3.1. Characterization of active oxygen species produced electrochemically

Different oxidation currents were applied to the Pt + carbon-mixed or pure Pt electrode in 3 vol% H_2O vapor diluted with argon at a temperature of 200 °C. Shown in Fig. 2 are the CO_2 and O_2 concentrations as a function of current, including the corresponding theoretical values calculated from Faraday's law based on a four-electron reaction. For the pure Pt electrode, the formation of O_2 was observed, and the O_2 concentration was in agreement with the theoretical value at each current. These results indicate that H_2O vapor is oxidized to protons and electrons as shown in Eq. (3):

$$2H_2O \rightarrow 4H^+ + 4e^- + O_2 \quad (3)$$

For the Pt + carbon-mixed electrode, however, CO_2 rather than O_2 was produced exactly according to Faraday's law, which is interpreted as indicative that carbon oxidation proceeded as in Eq. (1).

To further demonstrate the characteristics of electrochemical carbon oxidation over the Pt + carbon-mixed electrode, analysis of oxidation products was carried out at various temperatures. Shown in Fig. 3 is the CO_2 concentration as a function of current in the temperature range 50–300 °C, including the theoretical values calculated from Faraday's law based on a four-electron equation. Both CO_2 and O_2 were produced as oxidation products, with the proportion of each dependent on the temperature. The CO_2 concentration became closer to the theoretical value at each current as the temperature increased. In particular, at 200 °C or higher, CO_2 was formed with a current efficiency of 100% within experimental error. It is important to remember that TG and DTA analyses of the pure carbon sample showed that its ignition temperature was at least 500 °C in air (Fig. 4). These results confirm that electrochemical carbon oxidation very effectively occurs even at temperatures below 300 °C, consistent with the results of many research groups [11–16]. On the other hand, the presence of CO was not observed at all of the tested temperatures. It is likely that Pt plays a role in

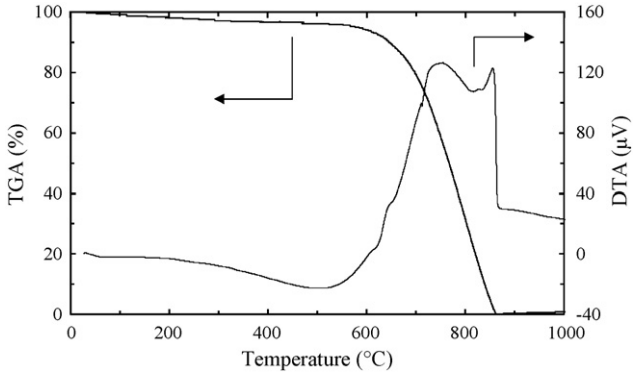

Fig. 4. Thermal stability of the carbon sample studied using TG and DTA. These analyses were carried out under air flow at a heating rate of 10 °C min^{-1}.

the oxidation of CO to CO_2, as reported by Willsau and Heitbaum [12].

CV measurements provided additional information on the above carbon oxidation over the Pt + carbon-mixed electrode. The CV profiles were measured in 3 vol% H_2O vapor diluted with argon from 50 to 300 °C. Fig. 5 shows that a large peak was detected between −0.3 and −0.5 V in the positive-direction scan at 200 °C or higher. These peaks are believed to be due to the formation of carbon surface oxides and the subsequent oxidation to CO_2 expressed in Eqs.

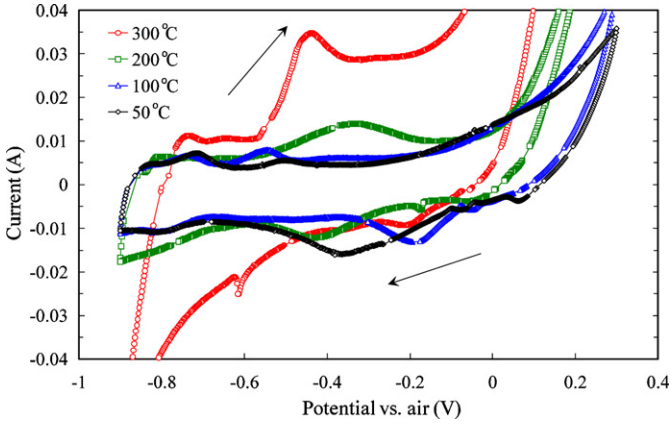

Fig. 5. CV curves observed for the Pt + carbon-mixed electrode in 3 vol% H_2O vapor diluted with argon at various temperatures. In this measurement, the Au reference electrode was exposed to ambient atmosphere.

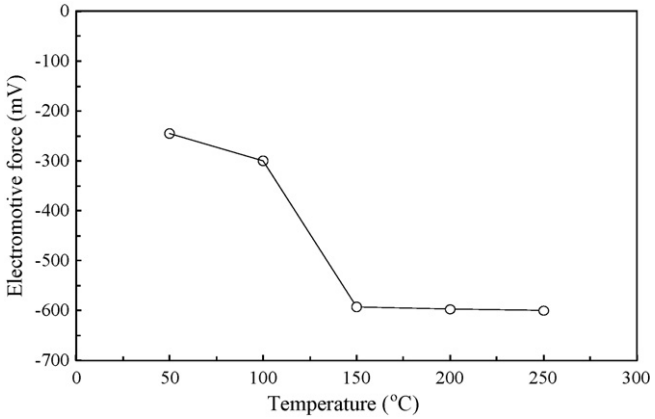

Fig. 6. EMF of the electrochemical cell comprised of 3 vol% H_2O vapor diluted with argon, Pt + carbon|$Sn_{0.9}In_{0.1}P_2O_7$|Pt, air at various temperatures.

(4) and (5) [13]:

$$C + H_2O \rightarrow C\text{–}O_{ad} + 2H^+ + 2e^- \quad (4)$$

$$C\text{–}O_{ad} + H_2O \rightarrow CO_2 + 2H^+ + 2e^- \quad (5)$$

Fig. 5 also shows a small peak in the range from −0.5 to −0.6 V, especially at 100 °C. This peak has been identified as resulting from the oxidation of CO adsorbed on the Pt surface to CO_2, according to Eq. (6) [12]:

$$Pt\text{–}CO_{ad} + H_2O \rightarrow Pt + CO_2 + 2H^+ + 2e^- \quad (6)$$

Although it is not clearly understood at the present time precisely how Pt catalyzes these reactions, the results suggest that the carbon oxidation to CO_2 shown in Figs. 2 and 3 mainly occurs as described in Eqs. (4) and (5). In addition, it is speculated that at temperatures below 200 °C, Pt catalyzes oxidation of CO to CO_2 via Eq. (6).

3.2. Formation of a local electrochemical cell

Importantly, CV measurements also revealed that the current peak due to the reactions shown in Eqs. (4) and (5) was seen at lower potentials than that (0 V in Fig. 5) based on the reaction represented by Eq. (3). Thus, it is expected that a fuel cell can be made up of the reactions in Eqs. (4) and (5) at the anode and the reaction in Eq. (3) at the cathode, as displayed in Scheme 1a. Carbon oxidation would spontaneously proceed by short circuiting the cell. Indeed, Fig. 6 shows that an electrochemical cell comprised of 3 vol% H_2O vapor diluted with argon, Pt + carbon|$Sn_{0.9}In_{0.1}P_2O_7$|Pt, air generated large electromotive forces ranging from 250 to 600 mV. This type of fuel cell is commonly regarded as a direct carbon fuel cell [19–21].

It is believed that both anodic and cathodic sites are present on the same electrode surface due to its heterogeneity at the atomic level [22]. If H_2O vapor and O_2 coexist in the reaction system, this structure enables the formation of a local electrochemical cell at the interface of the Pt + carbon-mixed electrode and the $Sn_{0.9}In_{0.1}P_2O_7$ electrolyte, as displayed in Scheme 1b. Consequently, carbon would be oxidized to CO_2 through the reactions shown in Eqs. (4) and (5) along with the reaction represented by Eq. (3), even in the half-cell. In this case, these reaction rates should be equal to each other due to the self-discharge, resulting in the appearance of a mixed potential at the Pt + carbon-mixed electrode [23–25].

To clarify this assumption, we estimated the mixed potentials from the polarization curves for H_2O vapor oxidation corresponding to the reactions in Eqs. (4) and (5) and for oxygen reduction corresponding to the reaction in Eq. (3), and compared them with the open-circuit potentials of the Pt + carbon-mixed electrode in a mixed feed of H_2O vapor and O_2. Shown in Fig. 7a as an example are the anodic polarization curve of 3 vol% H_2O vapor diluted with argon and the cathodic polarization curve of 21 vol% O_2 diluted with argon, both at 200 °C, wherein the direction of the cathodic current was reversed symmetrically with respect to the *x*-axis. The intersection point of the anodic and cathodic polarization curves, which corresponds to the mixed potential, was at −417 mV, which is in very good agreement with the open-circuit potential value of −417 mV measured at the Pt + carbon-mixed electrode in the 3 vol% H_2O vapor and 21 vol% O_2 mixture. Similar agreements between the mixed potentials and the open-circuit potentials at various temperatures are seen in Fig. 7b, demonstrating that the reactions in Eqs. (3)–(5) actually occur at the electrode in the presence of H_2O vapor and O_2. Further evidence is provided by the comparison of the short-circuit current values estimated from the intersection points of the polarization curves with the short-circuit current values cal-

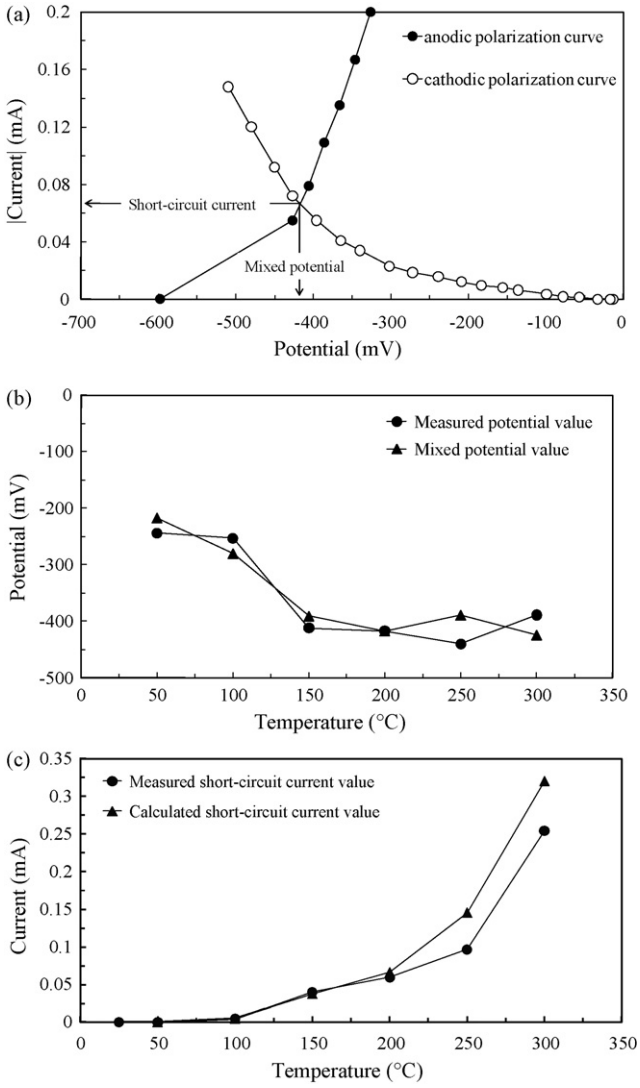

Fig. 7. (a) Anodic polarization curve for 3 vol% H_2O vapor diluted with argon over the Pt + carbon-mixed electrode and cathodic polarization curve for 21 vol% O_2 diluted with argon over the Pt electrode, both at 200 °C. The direction of the cathodic current is reversed. (b) Mixed potential estimated from the intersection points of the anodic and cathodic polarization curves and open-circuit potentials of the Pt + carbon-mixed electrode. (c) Short-circuit current estimated from the intersection points of the anodic and cathodic polarization curves and short-circuit current calculated from the CO_2 formation rate over the Pt + carbon-mixed electrode. The open-circuit potentials and the CO_2 formation rates were obtained in a 3 vol% H_2O vapor and 21 vol% O_2 mixture.

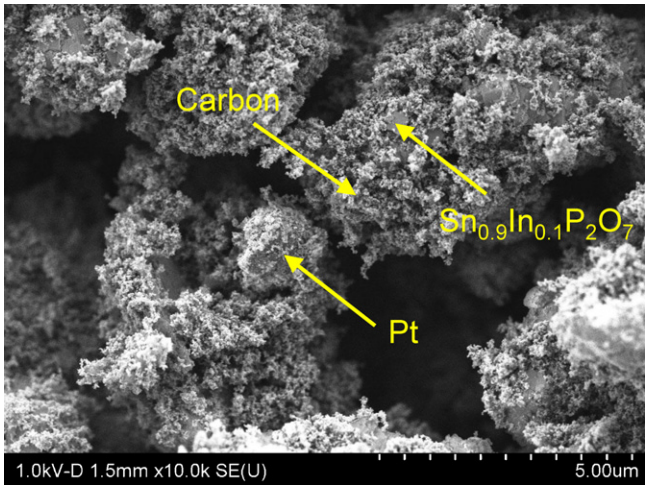

Fig. 8. SEM and EDX characterizations of the $Sn_{0.9}In_{0.1}P_2O_7$ + Pt + carbon mixture.

culated from the CO_2 formation rates over the Pt + carbon-mixed electrode in the presence of H_2O vapor and O_2. It can be seen from Fig. 7c that rough agreement between the two short-circuit current values is observed.

3.3. Carbon oxidation over $Sn_{0.9}In_{0.1}P_2O_7$ + Pt-mixed powders

Use of the mixed potential mechanism allows for the spontaneous formation of the active oxygen species and the subsequent oxidation of carbon in a H_2O and O_2 mixture. However, the electrochemical cell inherently shows a much smaller reaction area than conventional solid catalysts. We next attempted to increase the reaction area for carbon oxidation by mixing the $Sn_{0.9}In_{0.1}P_2O_7$ and Pt powders with the carbon powder in a mortar. Fig. 8 shows the results of SEM and EDX analysis of the mixed matrix. It can be seen that Pt aggregates, several microns in size, are interspersed between the $Sn_{0.9}In_{0.1}P_2O_7$ and carbon particles. The activity of the $Sn_{0.9}In_{0.1}P_2O_7$ + Pt-mixed catalyst for carbon oxidation was measured from room temperature to 600 °C in the 3 vol% H_2O vapor and 21 vol% O_2 mixture in argon. The results are shown in Fig. 9 along with the data for the individual materials as well as in the absence of a catalyst. For comparison, data for a Pt/γ-Al_2O_3 catalyst (1 wt% Pt) is also shown. The ignition temperature for the $Sn_{0.9}In_{0.1}P_2O_7$, Pt and Pt/γ-Al_2O_3 catalysts was 350 °C, which is slightly lower than the ignition temperature of 400 °C for non-catalytic carbon oxidation. In contrast, the ignition temperature for the $Sn_{0.9}In_{0.1}P_2O_7$ + Pt-mixed catalyst was drastically reduced to

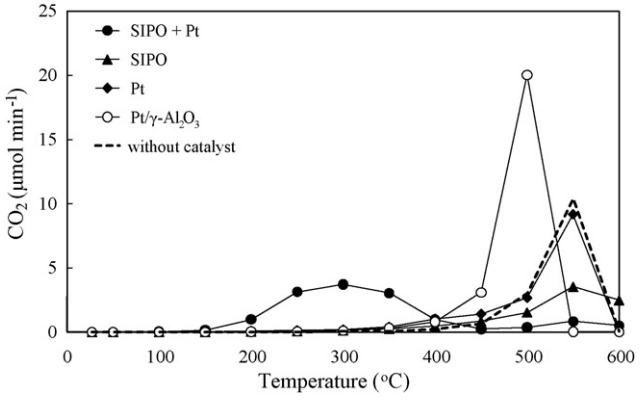

Fig. 9. Formation rates of CO_2 over various catalysts in a 3 vol% H_2O vapor and 21 vol% O_2 mixture.

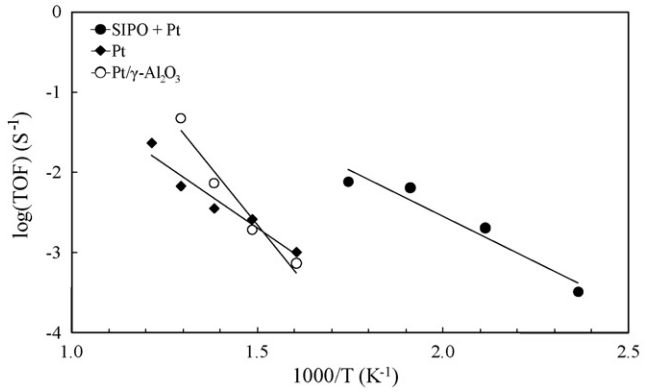

Fig. 10. TOFs for $Sn_{0.9}In_{0.1}P_2O_7$ + Pt (10 wt% Pt), Pt (10 mg), and Pt/γ-Al_2O_3 (1 wt% Pt) catalysts. The number of reaction sites on the Pt surface was measured at room temperature by the CO pulse method.

200 °C. Even larger differences were observed in the temperature at which the CO_2 formation rate peaked (defined as T_{peak}); T_{peak} was 300 °C for $Sn_{0.9}In_{0.1}P_2O_7$ + Pt, 500 °C for Pt/γ-Al_2O_3, and 550 °C for $Sn_{0.9}In_{0.1}P_2O_7$ and Pt. On the other hand, while CO_2 was the major oxidation product over the $Sn_{0.9}In_{0.1}P_2O_7$ + Pt, Pt and Pt/γ-Al_2O_3 catalysts and in the absence of a catalyst, the formation of CO as well as CO_2 was remarkable over the $Sn_{0.9}In_{0.1}P_2O_7$ catalyst. This activity is responsible for the low peak for the CO_2 formation rate over the $Sn_{0.9}In_{0.1}P_2O_7$ catalyst, although the reason for CO formation is not fully explained.

Comparison of the turnover frequency (TOF) for the above catalysts is useful to evaluate in more detail their differences in catalytic activity. We estimated the TOF based on the number of reaction sites on the Pt surface, which was measured by the CO pulse method at room temperature. The temperature dependence of the TOF for Pt in the above catalysts, except $Sn_{0.9}In_{0.1}P_2O_7$, is shown in Fig. 10. The TOF for the $Sn_{0.9}In_{0.1}P_2O_7$ + Pt-mixed catalyst was found to be at least ten times higher than that for the Pt/γ-Al_2O_3 and Pt catalysts. Moreover, the $Sn_{0.9}In_{0.1}P_2O_7$ + Pt-mixed catalyst exhibited a considerably lower activation energy (43.9 kJ mol^{-1}) than the Pt/γ-Al_2O_3 catalyst (109 kJ mol^{-1}). Therefore, it is concluded that the $Sn_{0.9}In_{0.1}P_2O_7$ + Pt-mixed catalyst produces a highly active oxygen species for carbon oxidation. In addition, these results demonstrate that the formation of such an active oxygen species is first accomplished by combining $Sn_{0.9}In_{0.1}P_2O_7$ and Pt in a manner similar to that found in an electrochemical cell.

In order to gain more detailed insights into the above results, carbon oxidation was conducted over the $Sn_{0.9}In_{0.1}P_2O_7$ + Pt-mixed catalyst under various conditions. As can be seen from Fig. 11a, the ignition temperature for carbon decreased with increasing H_2O vapor concentration in the reactant gas. A possible explanation is that the reactions shown in Eqs. (4) and (5) are enhanced by the increase in H_2O vapor concentration. Alternatively, proton migration through the $Sn_{0.9}In_{0.1}P_2O_7$ bulk (shown in Scheme 1b) may also be enhanced by increasing the proton conductivity of $Sn_{0.9}In_{0.1}P_2O_7$ with H_2O vapor concentration; the proton conductivities at 250 °C were 0.19, 0.20 and 0.22 S cm^{-1} at H_2O vapor concentrations of 0.6, 3 and 10 vol%, respectively [17,18]. This point can be supported by measuring the H/D isotope effect on the activity of the mixed catalyst because the electrical resistance of proton conductors commonly increases when protons are replaced with deuterons [26]. As shown in Fig. 11b, the ignition temperature for carbon was evidently increased when H_2O vapor was replaced with D_2O vapor, which suggests that carbon oxidation over the mixed catalyst relies on proton migration through the $Sn_{0.9}In_{0.1}P_2O_7$ bulk as well as the reactions in Eqs. (4) and (5).

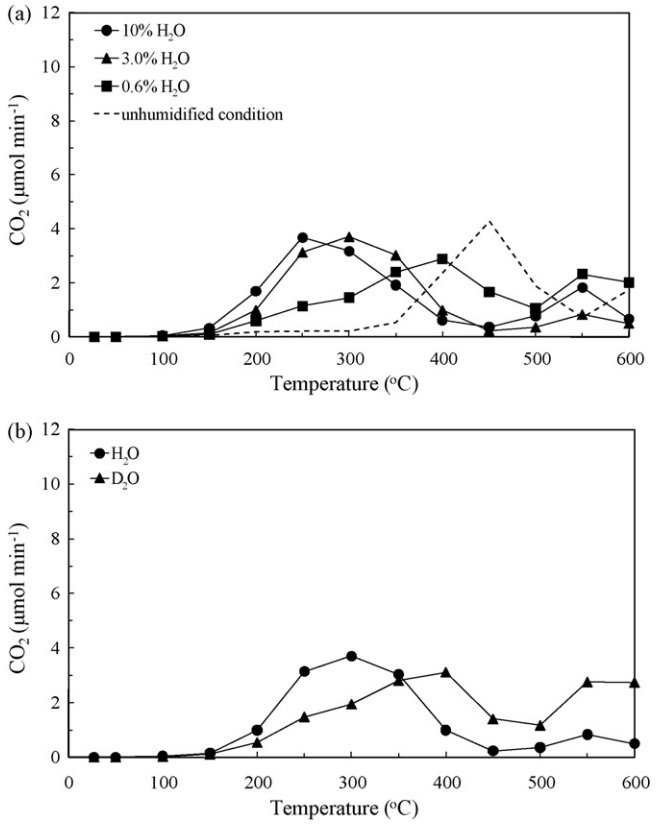

Fig. 11. Formation rates of CO_2 over the $Sn_{0.9}In_{0.1}P_2O_7$ + Pt-mixed catalyst (a) in an unhumidified 21 vol% O_2 or 0.6–10 vol% H_2O vapor and 21 vol% O_2 mixture and (b) in the 3 vol% D_2O vapor and 21 vol% O_2 mixture.

Based on the above results, it is expected that the present catalyst could be a promising candidate material for low-temperature soot combustion. There still remains, however, the need to use expensive Pt to achieve high activity for carbon oxidation. As part of a previous study to identify alternative materials to Pt in fuel cells, we found that Mo_2C showed the best anode performance among all tested metal carbides, M × C (M = Al, Si, Ti, Zr, Mo and W) [27,28]. Thus, an attempt was made to use Mo_2C in place of Pt for carbon oxidation. As can be seen in Fig. 12, the $Sn_{0.9}In_{0.1}P_2O_7$ + Mo_2C-mixed catalyst lowered the ignition temperature for carbon to 300 °C, which is slightly higher than the ignition temperature for the Pt-catalyzed oxidation, but considerably lower than the ignition temperature for non-catalytic oxidation. The unique catalytic

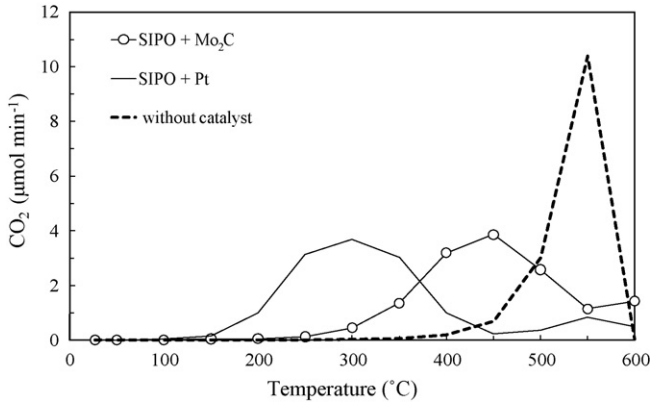

Fig. 12. Formation rate of CO_2 over the $Sn_{0.9}In_{0.1}P_2O_7$ + Mo_2C-mixed catalyst in 3 vol% H_2O vapor and 21 vol% O_2 mixture.

activity of Mo_2C can be explained by the change in the electron density of the d-band of Mo upon its carburization; the introduction of C atoms into the Mo metal lattice causes a contraction of the d-band, thus enhancing the d-electron density to the d-electron density levels of Pt [29]. Replacing Pt with Mo_2C is also a practical benefit to sulfur-containing diesel fuels because Mo_2C shows higher tolerance toward sulfidation than Pt [30]. However, diesel particulate matter includes SOF and other adsorbed species, which may inhibit soot oxidation. Further studies are needed to clarify the influence of such inhibitors on the oxidation activity.

4. Conclusions

The present study has proposed a concept for the formation of active oxygen from H_2O vapor at the proton conductor–electrocatalyst interface and has explored low-temperature carbon combustion using this active oxygen. $Sn_{0.9}In_{0.1}P_2O_7$ and Pt were used as the proton conductor and electrocatalyst, respectively. The carbon was oxidized to CO_2 by the electrolysis of H_2O vapor at 50 °C or higher, with the CO_2 formation rate reaching the theoretical values calculated from Faraday's law at 200 °C. The CV measurement showed that the active oxygen was formed over the carbon, depending on the electrode potential. The electrochemical activation of oxygen also occurred under open-circuit conditions when both H_2O vapor and O_2 were present in the reaction system. This phenomenon was further applicable to the $Sn_{0.9}In_{0.1}P_2O_7$ + Pt-mixed catalyst. The activity of the $Sn_{0.9}In_{0.1}P_2O_7$ + Pt-mixed catalyst for carbon oxidation was enhanced by the increase in H_2O vapor concentration, such that the ignition temperature for carbon was reduced to 200 °C. Finally, we emphasize that Pt in the $Sn_{0.9}In_{0.1}P_2O_7$ + Pt-mixed catalyst can be replaced with Mo_2C.

Acknowledgments

Dr. Satoshi Nagao, Dr. Hirohito Hirata and Dr. Shin-ichi Matsumoto (Toyota Motor Corporation) are acknowledged for providing a Pt/γ-Al_2O_3 catalyst.

References

[1] B.R. Stanmore, J.F. Brilhac, P. Gilot, Carbon 39 (2001) 2247–2268.
[2] B.A.A.L. van Setten, M. Makkee, J.A. Moulijn, Catal. Rev. 43 (2001) 489–564.
[3] M.V. Twigg, Appl. Catal. B 70 (2007) 2–15.
[4] G.C. Koltsakis, A.M. Stamatelos, Prog. Energy Combust. Sci. 23 (1997) 1–39.
[5] P.G. Harrison, I.K. Ball, W. Daniell, P. Lukinskas, M. Céspedes, E.E. Miró, M.A. Ulla, Chem. Eng. J. 95 (2003) 47–55.
[6] D. Uner, M.K. Demirkol, B. Dernaika, Appl. Catal. B 61 (2005) 334–345.
[7] F.S. Toniolo, E. Barbosa-Coutinho, M. Schwaab, I.C.L. Leocadio, R.S. Aderne, M. Schmal, J.C. Pinto, Appl. Catal. A 342 (2008) 87–92.
[8] A. Bueno-López, K. Krishna, M. Makkee, J.A. Moulijn, J. Catal. 230 (2005) 237–248.
[9] J. Liu, Z. Zhao, C. Xu, A. Duan, L. Wang, S. Zhang, Catal. Commun. 8 (2007) 220–224.
[10] T. Masui, K. Koyabu, K. Minami, T. Egawa, N. Imanaka, J. Phys. Chem. C 111 (2007) 13892–13897.
[11] K. Kinoshita, J.A.S. Bett, Carbon 12 (1974) 525–533.
[12] J. Willsau, J. Heitbaum, J. Electroanal. Chem. 161 (1984) 93–101.
[13] E. Passalacqua, P.L. Antonucci, M. Vivaldi, A. Patti, V. Antonucci, N. Giordano, K. Kinoshita, Electrochim. Acta 37 (1992) 2725–2730.
[14] S.D. Knights, K.M. Colbow, J. St-Pierre, D.P. Wilkinson, J. Power Sources 127 (2004) 127–134.
[15] K.H. Kangasniemi, D.A. Condit, T.D. Jarvi, J. Electrochem. Soc. 151 (2004) E125–E132.
[16] S. Maass, F. Finsterwalder, G. Frank, R. Hartmann, C. Merten, J. Power Sources 176 (2008) 444–451.
[17] M. Nagao, A. Takeuchi, P. Heo, T. Hibino, M. Sano, A. Tomita, Electrochem. Solid-State Lett. 9 (2006) A105–A109.
[18] M. Nagao, T. Kamiya, P. Heo, A. Tomita, T. Hibino, M. Sano, J. Electrochem. Soc. 153 (2006) A1604–A1609.
[19] M. Ihara, K. Matsuda, H. Sato, C. Yokoyama, Solid State Ionics 175 (2004) 51–54.
[20] S.L. Jain, Y. Nabae, B.J. Lakeman, K.D. Pointon, J.T.S. Irvine, Solid State Ionics 179 (2008) 1417–1421.

[21] S. Li, A.C. Lee, R.E. Mitchell, T.M. Gür, Solid State Ionics 179 (2008) 1549–1552.
[22] N. Miura, G. Lu, N. Yamazoe, H. Kurosawa, M. Hasei, J. Electrochem. Soc. 143 (1996) L33–L36.
[23] R. Mukundan, R.E. Brosha, D.R. Brown, F.H. Garzon, Electrochem. Solid-State Lett. 2 (1999) 412–414.
[24] X. Li, G.M. Kale, Sens. Actuators B 123 (2007) 254–261.
[25] A. Tomita, T. Yoshii, S. Teranishi, M. Nagao, T. Hibino, J. Catal. 247 (2007) 137–144.
[26] A.S. Nowick, A.V. Vaysleyb, Solid State Ionics 97 (1997) 17–26.
[27] P. Heo, M. Nagao, M. Sano, T. Hibino, J. Electrochem. Soc. 154 (2007) B53–B56.
[28] P. Heo, K. Ito, A. Tomita, T. Hibino, Angew. Chem. Int. Ed. 47 (2008) 7841–7844.
[29] J.S. Choi, G. Bugli, G. Djega-Mariadassou, J. Catal. 193 (2000) 238–247.
[30] P. Da Costa, J.-L. Lemberton, C. Potvin, J.-M. Manoli, G. Perot, M. Breysse, D. Djega-Mariadassou, Catal. Today 65 (2001) 195–200.